

# PET Imaging performance of a Dedicated Breast PET-DBT (BPET-DBT) scanner

Srilalan Krishnamoorthy, *Senior Member, IEEE*, Emmanuel Morales, William J. Ashmanskas, Matthew E. Werner, Trevor L. Vent, Andrew D.A. Maidment, Joel S. Karp, *Fellow, IEEE* and Suleman Surti, *Senior Member, IEEE*

**Abstract** – Our group at the University of Pennsylvania has designed and built a dedicated high spatial resolution time-of-flight (TOF)-capable breast PET (BPET) scanner integrated with a digital breast tomosynthesis (DBT) unit in a common gantry to provide co-registered PET-DBT images. The BPET scanner is comprised of two detector heads, with each head composed of a 4x2 array of PET detectors built using 1.5x1.5x15 mm<sup>3</sup> LYSO crystals. The PET detector head separation is set to 9 cm, providing a PET FOV of 20x9x10 cm<sup>3</sup>. In comparison with conventional dual-headed PET scanners, TOF information will help in alleviating limited-angle image artifacts and improve lesion quantification. This dedicated scanner will thus provide the ability to more accurately measure radiotracer uptake in smaller lesions that are prevalent in breast cancer. A custom data acquisition system performs fast signal waveform sampling at 4 Gbps with minimal deadtime. This paper describes the full system design and presents early imaging performance of the BPET scanner. In particular, results from reconstructed spatial resolution and phantom measurements are presented.

## I. INTRODUCTION

OUR group at the University of Pennsylvania has designed and built a dedicated high spatial resolution time-of-flight (TOF)-capable breast PET scanner. The PET scanner will be combined with a state-of-the-art digital breast tomosynthesis (DBT) [1] unit in an integrated gantry providing spatially co-registered 3D PET-DBT images. In comparison with conventional dual-headed PET scanners which suffer from image artifacts & reduced quantitation accuracy, TOF information will alleviate these effects and improve lesion quantification. We have previously described the design and performance of the PET detector [2], and DRS4 [3] based custom waveform-sampling electronics (ROCSTAR) and data acquisition [4] developed specifically to instrument this TOF PET scanner. This paper presents the PET-DBT scanner architecture and early imaging performance of the dedicated breast PET (BPET) scanner.

## II. MATERIALS AND METHODS

The PET scanner comprises of two detector heads, with each head comprising a 4x2 arrangement of PET detectors [2] using 1.5x1.5x15 mm<sup>3</sup> LYSO crystals. The detector heads are separated by 9 cm, providing a 20 (X) x 9 (Y) x 10 (Z) cm<sup>3</sup>

FOV. With a modular PET detector and waveform sampling electronics, the entire scanner comprises of 16 PET detectors and ROCSTAR boards. A separate external board is used to detect & only read-out coincidence events within a 5 ns coincidence window. The DBT is a next-generation system that supports advanced x-ray tube and detector motion to improve DBT image quality. *Fig. 1* shows the PET-DBT scanner. As shown in *Fig. 1 left*, during DBT imaging, the PET detectors are retracted away from the x-ray source. Immediately after the DBT acquisition, the x-ray detector is retracted, the PET detectors are moved into position and the PET acquisition begins with the breast in the same compressed position (*Fig. 1 right*). The design thus provides intrinsically co-registered PET and DBT images.

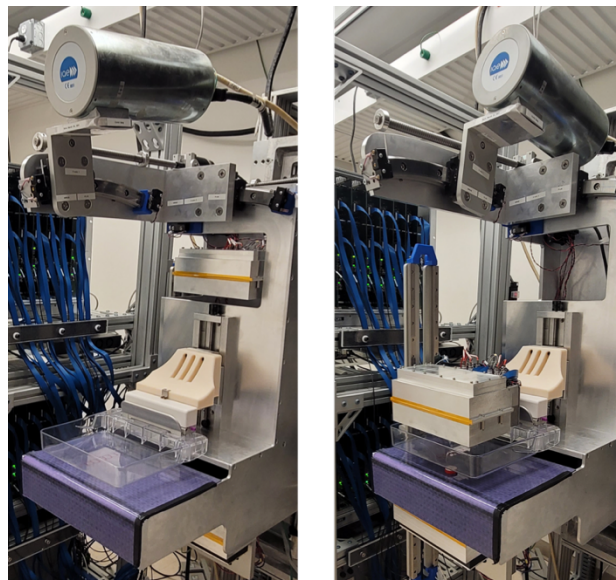


*Fig. 1.* PET-DBT scanner in DBT-imaging mode (*left*) and PET imaging mode (*right*). The PET detector heads (pictured with yellow band) are retracted-back during DBT-imaging, and pulled-forward during PET-imaging. During the entire process the breast continues to be held under milder clinical compression by the breast compression paddle (plexiglass paddle below the top PET detector head on *right*).

PET scanner spatial resolution was measured using an ~1.15mm diameter <sup>18</sup>F<sup>18</sup>FDG-filled capillary that was ~2.5 cm

Manuscript received December 1, 2021. The work was supported by National Institutes of Health R01CA196528, R01CA113941, R01EB028764 & R21CA239177, Komen Foundation (IIR13264610), and Burroughs Wellcome Foundation (IRSA 1016451) grants.

S. Krishnamoorthy (srilalan@pennmedicine.upenn.edu), M.E. Werner, A.D.A. Maidment and S. Surti are with the Dept. of Radiology at the University of Pennsylvania, Philadelphia, PA, USA. E. Morales, and W.J. Ashmanskas are

with the Dept. of Physics and Astronomy at the University of Pennsylvania, Philadelphia, PA, USA. T. Vent is with the Dept. of Bioengineering at the University of Pennsylvania, Philadelphia, PA, USA. J.S. Karp is with the Depts. of Radiology and Physics & Astronomy at the University of Pennsylvania, Philadelphia, PA, USA.

long. First imaging test was performed with an  $^{18}\text{F}$ FDG-filled Micro-Deluxe hot rod Derenzo phantom that has rods ranging from 1.2 to 4.8 mm in diameter [6].

During PET acquisition, raw data from all individual ROCSTAR boards are transmitted over a Gigabit link to the DAQ computer. All data processing is performed offline using custom MATLAB/C code that parses raw DAQ data and generates list-mode PET data that is reconstructed with  $1\text{ mm}^3$  voxels using a blob-based iterative TOF reconstruction program [5] utilizing a 700 ps FWHM Gaussian kernel. Detector and scanner calibrations were performed using an  $^{18}\text{F}$ FDG filled uniform sheet source placed between the two PET detector heads.

### III. RESULTS, DISCUSSION & SUMMARY

Fig. 2 shows a single slice from reconstruction of the  $^{18}\text{F}$ FDG filled capillary. Both transverse and coronal slices are shown. Also shown is a profile along the X-direction of the scanner. Keeping in mind the capillary size, the  $\sim 2\text{mm}$  FWHM is commensurate with the 1.5mm-wide LYSO crystals used in the scanner. Along the Y-direction, there is additional blurring due to partial angular coverage effects that are not fully mitigated by the 700ps TOF kernel currently being used for image reconstruction. The overall scanner timing resolution is presently influenced by some additional jitter in board-to-board pulse-timing synchronization, which we suspect can be attributed to our waveform-sampling timing-calibration software. We are working on reducing this jitter and lowering the overall scanner timing resolution to the intrinsic detector timing resolution of  $\sim 400\text{ ps}$  [4]. Fig. 3 shows a Coronal image slice from the Micro-Deluxe hot rod Derenzo phantom. The 2.4 mm diameter rods are clearly visible.

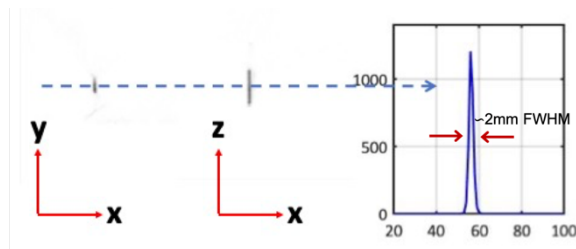


Fig. 2. Transverse and Coronal image slice from imaging a  $\sim 1.15\text{mm}$  diameter  $^{18}\text{F}$ FDG-filled capillary and transverse profile through the image slice. The capillary was placed  $\sim 5\text{ cm}$  away from the center of the PET scanner FOV.

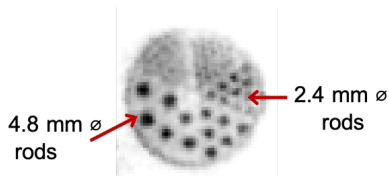


Fig. 3. Coronal image of the Micro-Deluxe hot rod Derenzo phantom.

To summarize, a high spatial resolution TOF-capable dedicated breast PET scanner has been built and integrated with a next-generation DBT scanner. Both scanners are fully operational and first phantom studies have been performed. Some system calibrations (especially system timing resolution) are still ongoing and are expected to improve scanner

performance. These will be completed before characterizing full scanner performance and commencing patient studies.

### ACKNOWLEDGMENT

Authors acknowledge support from the Cyclotron facility in the PET Center of the Department of Radiology. We also acknowledge Mitch Newcomer and R. Van Berg from the Physics and Astronomy department for advice pertaining to data acquisition development.

### REFERENCES

- [1] T.L. Vent, B. Barufaldi, R.J. Acciavatti, S. Krishnamoorthy, S. Surti and A.D.A. Maidment, "Next generation tomography image acquisition optimization for dedicated PET-DBT attenuation corrections," Proc. SPIE 11595, Medical Imaging 2021: Physics of Medical Imaging, 115954V.
- [2] S. Krishnamoorthy, B.C. LeGeyt, M.E. Werner, M. Kaul, F.M. Newcomer, J.S. Karp and S. Surti, "Design and performance of a high spatial resolution, time-of-flight PET detector," IEEE Transactions on Nuclear Science, vol. 61, no. 3, pp. 1092-1098, 2014.
- [3] S. Ritt, R. Dinapoli and U. Hartmann, "Application of the DRS chip for fast waveform sampling," Nuclear Instruments and Methods in Physics Research Section A, vol. 623(1), pp. 486-488, 2010.
- [4] S. Krishnamoorthy, E. Morales, W.J. Ashmanskas, G. Mayers, F.M. Newcomer, J.S. Karp and S. Surti, "Coincidence Imaging with a custom-built waveform sampling data acquisition system for time-of-flight PET," 2020 IEEE Nuclear Science Symposium and Medical Imaging Conference (NSS/MIC), 2020, pp. 1-3.
- [5] S. Krishnamoorthy, T. Vent, B. Barufaldi, A.D.A. Maidment, J.S. Karp and S. Surti, "Evaluating attenuation correction strategies in a dedicated, single-gantry breast PET-tomography scanner," Phys. Med. Biol., 65(23) 235028, 2020.
- [6] <https://www.spect.com/our-products/preclinical/micro-deluxe-phantom/>